# Selection and stabilization of spatiotemporal patterns in two-dimensional coupled map lattices

Yu Jiang,[1,2] A. Antillón,[3] P. Parmananda,[1] and J. Escalona[1]

[1]*Facultad de Ciencias, Universidad Autónoma del Estado de Morelos, Avenida Universidad No. 1001, Caixa Postal 62210, Cuernavaca, Morelos, Mexico*

[2]*Departamento de Física, Universidad Autónoma Metropolitana–Iztapalapa, Apartado Postal 55-534, 09340 Mexico, Distrito Federal, Mexico*

[3]*Instituto de Física, Laboratorio de Cuernavaca, Universidad Nacional Autónoma de México, Apartado Postal 48-3, 62251 Cuernavaca, Morelos, Mexico*

(Received 14 January 1997)

A method for the stabilization and manipulation of stable and unstable spatiotemporal patterns of a coupled map lattice is presented. The selection of stable pattern states and the stabilization of unstable ones are achieved by using nonlinear feedback that contains the structural and dynamical information of the target patterns. The feedback vanishes once the spatiotemporal pattern is stabilized or selected.
[S1063-651X(97)00909-4]

PACS number(s): 05.45.+b, 47.54.+r, 82.40.Bj

The pattern-forming phenomena in spatially extended systems have attracted much attention recently [1–5]. Such systems often exhibit turbulence or spatiotemporal chaos (STC), in which many stable and unstable regular modes of spatiotemporal patterns are embedded. In many cases, however, it is desirable to make complex systems operate in highly nonlinear regimes while retaining certain temporal and/or spatial coherence. Recently, there have been reports of stabilizing unstable patterns in spatially extended systems [6–9]. The unstable states in such systems are typically high dimensional and involve multiple stable and unstable modes; therefore, simple control approaches are unable to stabilize a specified spatiotemporal pattern. In this paper we present a technique that allows us to select and stabilize such unstable states. Our method can be regarded as a generalization of the nonlinear feedback approach developed by Pyragas [10,11].

We consider a two-dimensional coupled map lattice (CML) [12–17]

$$x_{n+1}^{i,j}=(1-\epsilon)f(x_{n+1}^{i,j})+\frac{\epsilon}{4}[f(x_n^{i-1,j})+f(x_n^{i+1,j})+f(x_n^{i,j-1}) + f(x_n^{i,j+1})], \tag{1}$$

where $n$ is a discrete time step and $(i,j)$ denotes a two-dimensional lattice point ($i,j=1,2,\ldots,N$, where $N$ denotes the system size). The mapping function is chosen to be the logistic map $f(x)=ax(1-x)$. For convenience we introduce

$$F(\{\mathbf{x}_n\})=(1-\epsilon)f(x_{n+1}^{i,j})+\frac{\epsilon}{4}[f(x_n^{i-1,j})+f(x_n^{i+1,j}) + f(x_n^{i,j-1})+f(x_n^{i,j+1})],$$

where $\{\mathbf{x}_n\}$ represents a set of states including the state of site $(i,j)$ and its neighboring sites. Note that the function $F(\{\mathbf{x}_n\})$ contains all the information of a spatiotemporal state. Suppose that the target pattern is described by a spatiotemporal function $u_n^{i,j}$. Then our controlled system can be formally written as

$$x_{n+m}^{i,j}=F^m(\{\mathbf{x}_n\})-\gamma[F^m(\{\mathbf{x}_n\})-u_n^{i,j}], \tag{2}$$

where $\gamma$ is an empirically adjustable weight of the perturbation and $F^m(\{\mathbf{x}_n\})$ stands for the $m$th iteration of the function $F$. It follows immediately that once the system is controlled within the desired configuration characterized by $u_n^{i,j}$, the forcing term $\gamma[F^m(\{\mathbf{x}\})-u_n^{i,j}]$ vanishes. There are basically two types of control, depending on the nature of the forcing term: the external force control, where $u_n^{i,j}$ represents specially designed external coupled oscillators, and the delayed feedback control, where $u_n^{i,j}$ is a function of $x_{n-k}^{i,j}$ with $k$ being an arbitrary integer.

Spatiotemporal patterns can be classified in terms of the characteristic wave vector $q_0$ and frequency $\omega_0$ of the instability. Type-$I_s$ systems ($\omega_0=0$, $q_0\neq 0$) are stationary in time and periodic in space; type-$III_0$ systems ($\omega_0\neq 0$, $q_0=0$) and type-$I_0$ systems ($\omega_0\neq 0$, $q_0\neq 0$) are periodic in both space and time [1]. One of the major purposes of this work is to show that all three types of instabilities can be suppressed by using a nonlinear feedback control method. Since our interest is to control STC and select and stabilize an unstable spatiotemporal pattern in a two-dimensional CML, we take $a=4$ in all our numerical simulations, which corresponds to the fully developed chaos in the logistic map. It is interesting to note that even the dynamics of constituent elements is fully chaotic; for certain diffusive coupling $\epsilon$ there may exist stable spatiotemporal patterns of the coupled system, some of which may be reached after a long-time transient. Our method allows us to select those stable spatiotemporal patterns and study the dynamics of the coupled system near the instability threshold.

For illustration of our method, we restrict ourselves to the stabilization of two-state spatiotemporal patterns (STPs), where each individual site may either stay in one of the two

 

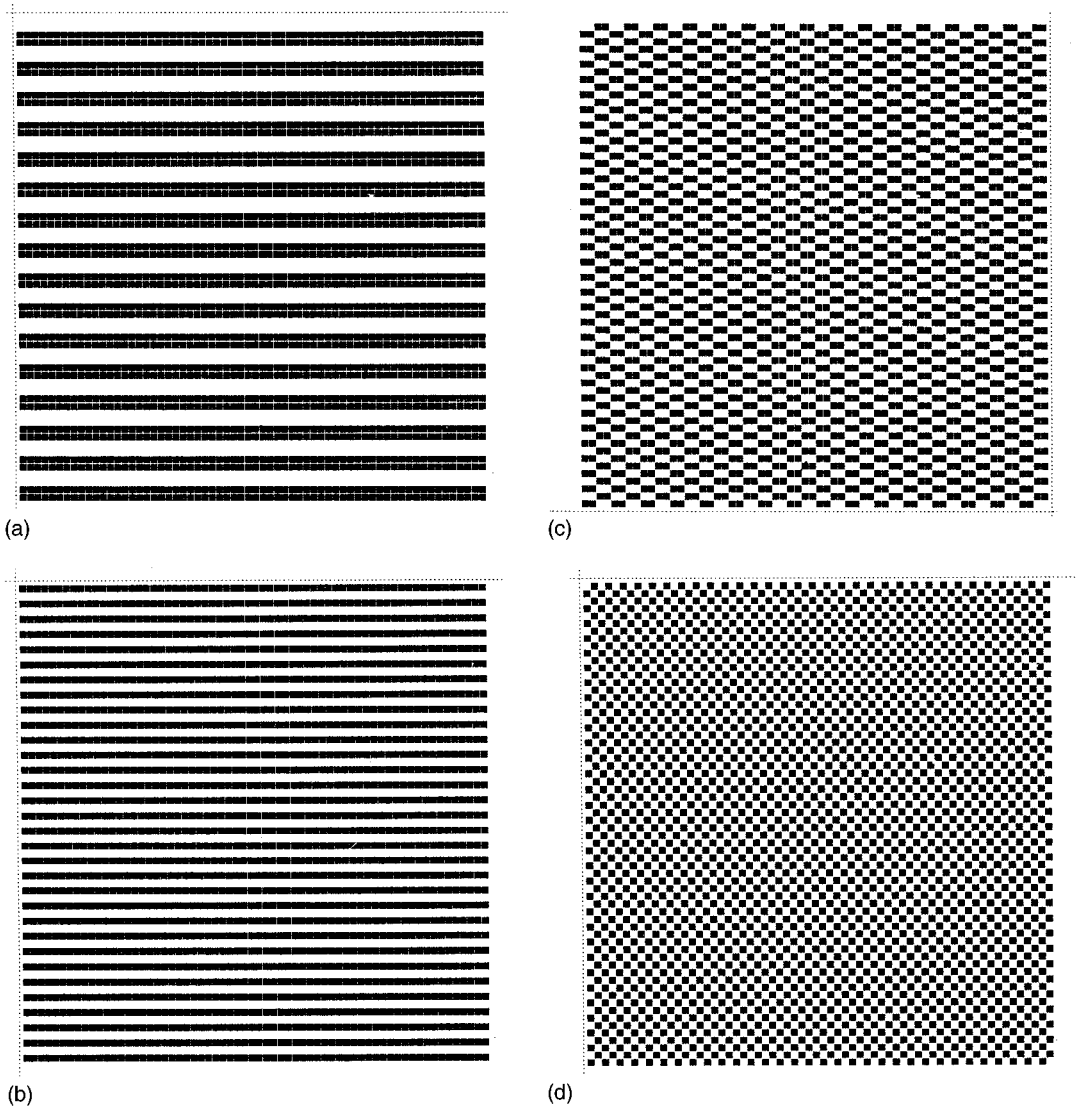


FIG. 1. Stabilized patterns in two-dimensional coupled map lattices. The nonlinearity of the logistic map is $a=4$ and the feedback strength is $\gamma=0.8$. The diffusive coupling is taken to be $\epsilon=0.1$, so that all pattern states are unstable. Here the solid squares represent the state $x_2$ and the open squares are for the state $x_1$. The parameter (a) $b=1$, (b) $b=2$, (c) $b=3$, and (d) $b=4$.

states or oscillate between these two states. Suppose that the two states are denoted by $x_1$ and $x_2$. To describe STPs, we introduce a parameter $b$, which represents the number of antiphase neighboring sites. For example, if the site $(i,j)$ is in the state $x_1$, then $b$ is the number of its neighboring sites that are in the state $x_2$. It is clear that for a square lattice $b\leqslant 4$. For stationary patterns, Eq. (1) can be reduced to

$$x_1=f(x_1)+\frac{b\epsilon}{4}[f(x_2)-f(x_1)],$$
$$x_2=f(x_2)+\frac{b\epsilon}{4}[f(x_1)-f(x_2)]. \tag{3}$$

For oscillatory (temporally period-2) patterns, one has

$$x_1=f(x_2)+\frac{b\epsilon}{4}[f(x_1)-f(x_2)],$$
$$x_2=f(x_1)+\frac{b\epsilon}{4}[f(x_2)-f(x_1)]. \tag{4}$$

The solutions to those equations with $f(x)$ being the logistic map are given by

$$x_1+x_2=\lambda,$$
$$x_1=\frac{\lambda}{2}\left[1+\sqrt{1-\frac{2}{\lambda a}(1-a+\lambda a)}\right], \tag{5}$$

where

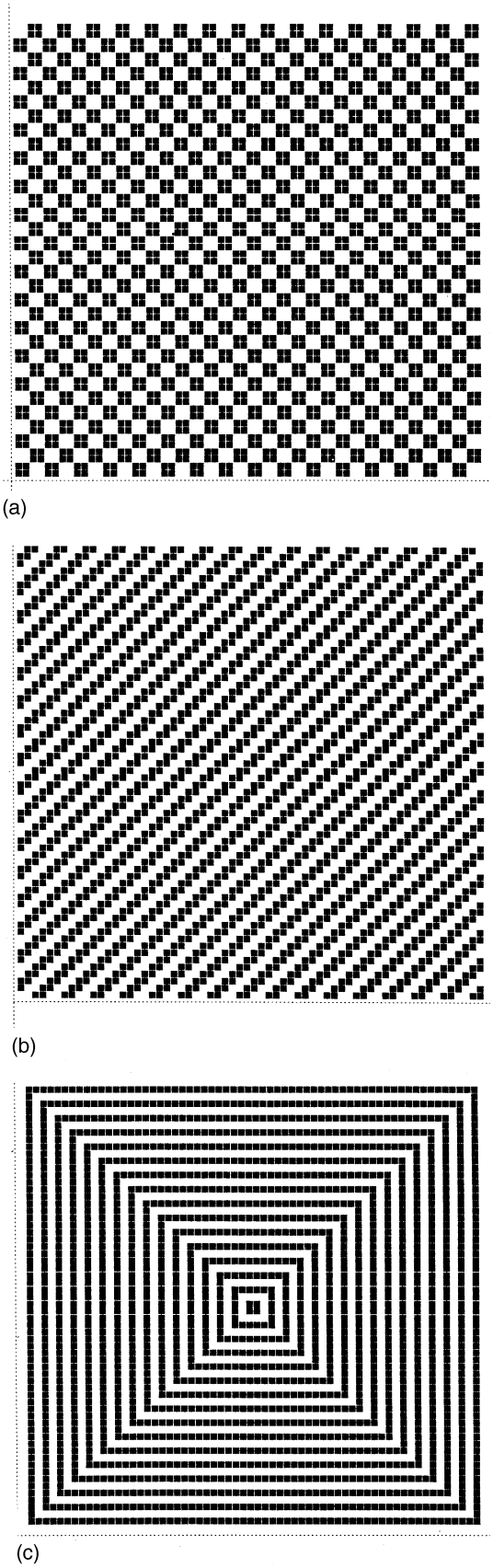


FIG. 2. Different stabilized patterns for $b=2$. Other parameter values are the same as in Fig. 1. Note that in obtaining the targetlike pattern (c) a time-dependent boundary condition, which is consistent with the oscillation pattern, is used; otherwise the periodic boundary condition is assumed.

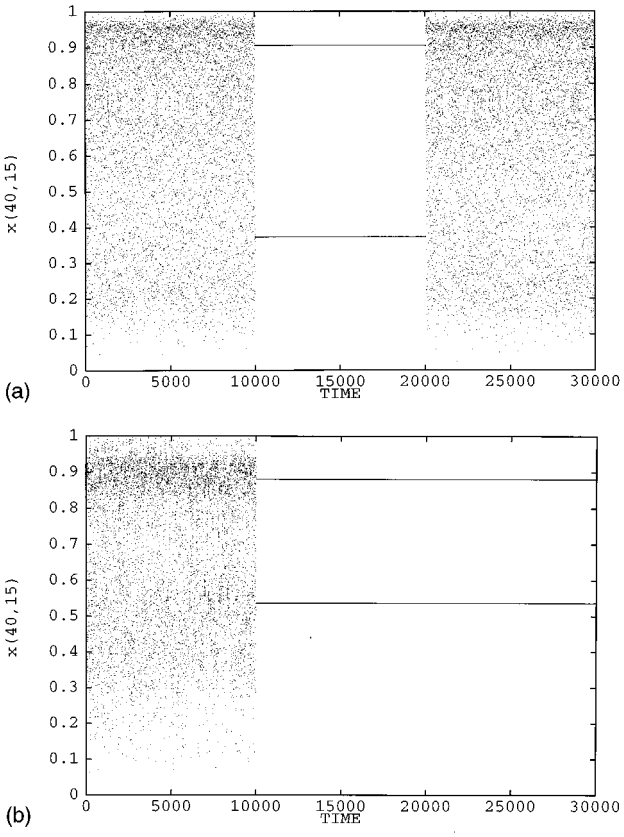


FIG. 3. Time evolution of some individual sit at (a) $\epsilon=0.1$ and (b) $\epsilon=0.4$. Other parameter values are the same as in Fig. 1.

$$\lambda=\begin{cases}1-\dfrac{1}{\left(1-\dfrac{b\epsilon}{2}\right)a} & \text{for stationary patterns}\\[2ex] 1+\dfrac{1}{\left(1-\dfrac{be}{2}\right)a} & \text{for oscillatory patterns.}\end{cases}\tag{6}$$

These solutions exist only in the parameter range

$$1<\lambda<2\left(1-\frac{1}{a}\right),\tag{7}$$

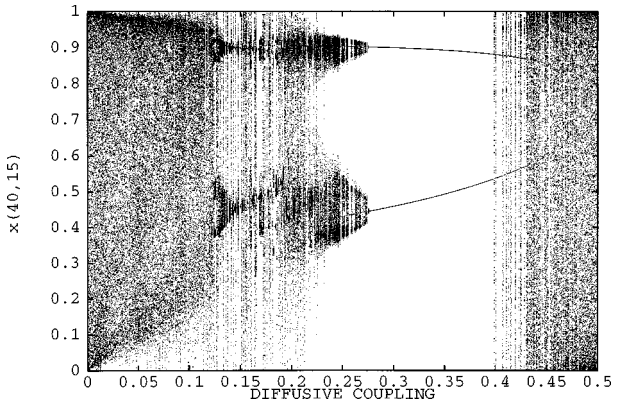


FIG. 4. Bifurcation diagram corresponding to the stripe pattern as shown in Fig. 2(c). This clearly shows that the stability of a spatiotemporal pattern varies with the diffusive coupling $\epsilon$.

which sets a restriction for the diffusive coupling $\epsilon$, i.e.,

$$\frac{2}{b}<\epsilon<\frac{2}{b}\left(1+\frac{1}{a-2}\right) \tag{8}$$

for stationary patterns and

$$0<\epsilon<\frac{2}{b}\left(1-\frac{1}{a-2}\right) \tag{9}$$

for oscillatory patterns. It should be emphasized that in this work we consider only the simple, regular STPs. A detailed analysis of more complicated patterns will be given elsewhere [18].

We performed numerical simulations of Eq. (2) on a two-dimensional square lattice with lattice size $N=64$. We used random values as initial states in all the numerical simulations of Eq. (2). Following Eq. (5), our control scheme for period-2 orbit can be written as

$$x_{n+2}^{i,j}=F^2(\{\mathbf{x}_n\})-\gamma[F^2(\{\mathbf{x}_n\})-x_{1,2}], \tag{10}$$

where $x_{1,2}$ are the two states in period-2 orbit, which are given by Eq. (5). The positions where the feedback is imposed are determined according to the target patterns. In general, it is enough to control only one of the two states. In Fig. 1 we show the stabilization of oscillatory two-state patterns for different $b$. The diffusive coupling is chosen such that the spatiotemporal patterns are unstable. That is, without application of the control, the system exhibits spatiotemporal chaos. The structure information is fed into the system through specially designed feedbacks. It is interesting to note that if a delayed feedback control like

$$x_{n+2}^{i,j}=F^2(\{\mathbf{x}_n\})-\gamma[F^2(\{\mathbf{x}_n\})-x_n^{i,j}], \tag{11}$$

is used instead, a checkerboard (spatiotemporal period-2) pattern will be selected and stabilized. It is obvious that for the same parameter $b$, there may exist many different spatial patterns. For example, in Fig. 2 it is seen that various spatial patterns corresponding to $b=2$ are stabilized. It should be remarked that all the spatiotemporal patterns shown in Fig. 2 are for the same values of system parameters and under the same initial and boundary conditions [except Fig. 2(c), where a time-dependent boundary condition is used]. The only difference is the feedback, which is designed according to different target patterns. Since the feedback vanishes when the control is achieved, the stabilized spatiotemporal pattern states are surely the solutions of the original system.

To illustrate the selection and stabilization of spatiotemporal patterns in a highly nonlinear system, we plot the time evolution of some individual site in Fig. 3. The control is turn on at iteration step 10 000 and turned off at 20 000. The spatiotemporal pattern under consideration is the stripelike pattern as shown in Fig. 1(b). We found that this state is stable at $\epsilon=0.4$ and unstable at $\epsilon=0.1$ (see Fig. 3). A bifurcation diagram is shown in Fig. 4, where the amplitude of site (40,15) is plotted against the diffusive coupling $\epsilon$ for the last 200 iterations after the control is turned off. The period-2 windows correspond to the stable stripelike pattern, while the chaotic regions indicate the destabilization of the once stabilized patterns. It is worthwhile to point out that the stripe pattern can be stabilized for all values of diffusive coupling $\epsilon$ over the range $0<\epsilon<0.5$. Figure 4 shows that as $\epsilon$ varies, transitions between stable and unstable stripe-pattern states occur alternatively, which seems to be a general feature of such pattern states.

In conclusion, we have presented a control method that allows the selection and stabilization of unstable spatiotemporal patterns. The method has been applied successfully to coupled map lattices and has allowed the determination of unstable pattern solution branches of the system. The technique is powerful, flexible, and robust against noise and allows the stabilization of any unstable pattern state under random initial conditions.

Our simulation results show that by using the chaos control method proposed in this work, one can manipulate the spatiotemporal patterns that are possible solutions of a spatially extended system, but are not observed under natural conditions. This could have enormous technological impact if such a manipulation can be realized in experiments. On the other hand, it may be assumed that in high-level life systems (e.g., the neural system) there may exist a recognition mechanism (associated with memory, for example) that can select and stabilize a recognized pattern from an apparently chaotic signal. Such a filter function might explain why a neural system behaves quite reasonably while an apparent chaostic signal is propagating through it. It is expected that much richer behaviors can be found if the manipulation idea is applied to other spatially extended systems, especially the reaction-diffusion system.

[1] M. C. Cross and P. C. Hohenberg, Rev. Mod. Phys. **65**, 851 (1993).
[2] A. J. Koch and H. Meihardt, Rev. Mod. Phys. **66**, 1481 (1994).
[3] A. T. Winfree, *The Geometry of Biological Time* (Springer, New York, 1980).
[4] A. T. Winfree, *When Times Breaks Down* (Princeton University Press, Princeton, 1987).
[5] Y. Kuramoto, *Chemical Oscillations, Waves, and Turbulence* (Springer-Verlag, Berlin, 1984).
[6] V. Petro, S. Metens, P. Borckmans, G. Dewel, and K. Showalter, Phys. Rev. Lett. **75**, 2895 (1995).
[7] A. Hagberg and E. Meron, Phys. Rev. Lett. **76**, 427 (1996).
[8] J. A. Sepulchre and A. Babloyantz, Phys. Rev. E **48**, 945 (1993).
[9] R. Martin, A. J. Scroggie, G.-L. Oppo, and W. J. Firth, Phys. Rev. Lett. **77**, 4007 (1996).
[10] K. Pyragas, Phys. Lett. A **170**, 421 (1992).
[11] M. de Sousa Vieira and A. J. Lichtenberg, Phys. Rev. E **54**, 1200 (1996).
[12] K. Kaneko, Physica D **34**, 1 (1989).

[13] K. Kaneko, Physica D **37**, 60 (1989).
[14] D. Keeler and J. D. Farmer, Physica D **23**, 413 (1986).
[15] J. P. Cruthfield and K. Kaneko, in *Directions in Chaos*, edited by Hao Bailin (World Scientific, Singapore, 1987).
[16] *Coupled Map Lattices: Theory and Experiments*, edited by K. Kaneko (World Scientific, Singapore, 1993).
[17] P. Marcq, H. Chate, and P. Manneville, Phys. Rev. Lett. **77**, 4003 (1996).
[18] Yu Jiang (unpublished).